International Journal of the Physical Sciences Vol. 5(7), pp. 1164-1174, July 2010
Available online at http://www.academicjournals.org/IJPS
ISSN 1992 - 1950 ©2010 Academic Journals

Full Length Research Paper

The structure behavior of reinforced concrete wing-wall under earthquake

Kuo-Chiang Liu[1,3] , Yuh-Wehn Liu[2] , Wen-Chun Huang[3] and Chen-Yuan Chen[4]*

[1]Department of Architectural Engineering, Yung-Ta Institute of Technology, Taiwan.
[2]Institute of Industrial Safety Disaster Provention, Chia-Nan University of Pharmacy and Science, Taiwan.
[3]Department of Architecture, National Cheng-Kung University, Taiwan.
[4]Department of Computer Science, National Pingtung University of Education, No. 4 - 18, Ming Shen Rd., Pingtung 90003, Taiwan.

Accepted 7 June, 2010

Lately, the applications to structural and mechanical systems are extensively reported using new approaches such as fuzzy, neural network, genetic algorism, etc. Under the earthquake hazard, many retrofitting ways of construction were contributed to the study. This study was done to investigate the characteristics of wing-wall to be used on retrofitting some damaged buildings during the earthquake. It included two main parts: Firstly, one specimen was made with a single column, according to ACI-code with 20 × 20 cm section, 135 cm in length, 8 - 4# main bars and #3 size hoops, which are the main observation parts. In another, one set added wings to each side of the main column with a 10 cm thickness and width as 10, 20, 30 and 40 cm specimens, while another set with a 15 cm thickness and width as 10 and 20 cm specimens were made to find out how the thickness and width of these wings were influenced. Two higher concrete compressive strength specimens were made to find out how the concrete strength influences the specimen. In another, two specimens with higher steel ratio (ρ) were made to see the influence of the steel ratio on the specimen. Secondly, the characteristics of materials theoretically analyzed were used reasonably in finding the test results that simulated the construction elements under the attack of earthquake. The model characteristic of wing-wall, the effective height factor (K) of wing-wall, the relationship between the width of wing-wall and the width of column are found in this study. Finally, good agreements were obtained from these test results and the theoretical analysis. This shows that the study is reliable. Consequently, the wing-wall to be used on retrofit damage constructions is accommodation.

Key words: Wing-wall, retrofit, effective factor, fuzzy, neural network, genetic algorism.

INTRODUCTION

Lately, the applications to structural and mechanical systems are extensively reported using new approaches, such as fuzzy, neural network, genetic algorism, etc (Chen, 2006; Chen et al., 2007; Chen, 2009; Chen et al., 2009; Chen et al., 2009; Chen, 2009; Chen et al., 2010; Chen, 2010; Chen et al., 2010; Chen and Chen, 2010). These indicate the important role of classical physical problems. The resistant of a construction under earthquake is needed for it not to suffer bending moment, shear force, normal loading and torsion in the mean time during earthquake. Actually, it is needed in daily life for a construction of convenience, comfortable air currency, lighting, brilliant, etc. It, without doubt, is further more important than later in the study's need. Wing-wall, which is an element of construction, is composed together with column and wings by the side. The wing-wall can be a good component of building element in strengthening both resistant shear and axial force in retrofitting conventional column. In shear wall, resistant shear force is the main performance with the room separated purpose, but causes the inconvenient performance to be used before setting it. Wing-wall just implements the missing performance with that of convenient and promotes the resistant force under earthquake. Based on the reason, our studies suggest changing the current design procedures to provide ductile behavior modes (Lefas et al., 1990; Lefas

*Corresponding author. E-mail: cyc@mail.npue.edu.tw.

and Kotsovos, 1990). Besides, we investigate the structure behavior of reinforced concrete wing –wall under seismic action.

FRAMEWORKS

Preparation and construction for specimen

The Figures 1-3 respectively show the scale of a wing-wall specimen, steel arrangement in wing-wall specimen, and test frame and hinge fixed bars for wing-wall. All parameters in the tests are list in the Table 1. After each test, the cures of P-△ as Figures 4-5 are plotted for analyses. Wing-wall specimens were made according to test plan and the course is as follows:

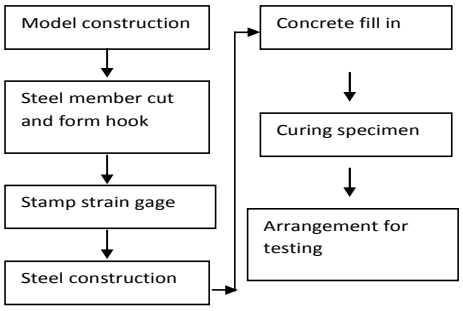

Test of specimen

The testing sequence steps show the following:

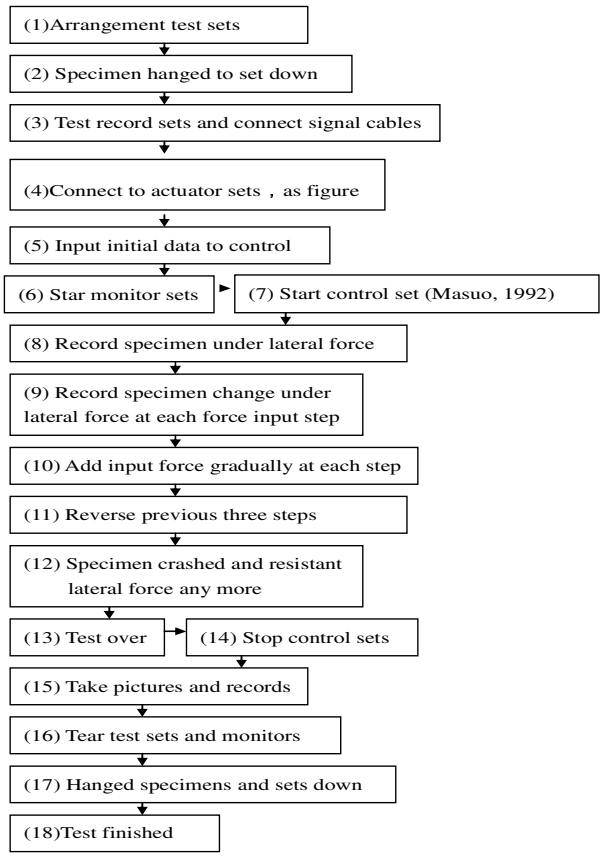

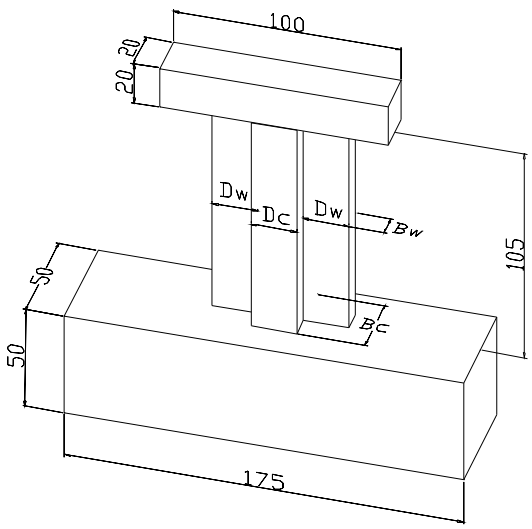

Figure 1a. Scale of a wing-wall specimen (unit : cm).

Figure 1b. Specimen of wing-wall.

THEORY FROM TEST RESULTS

Deformation behavior of rigidity frame analysis of wing-wall

Semi-rigid frame mode of wing-wall under lateral force

The specimen under external force reaction should be revealed as Figure 6. Actually, the inflection point is higher than the ideal point which should be in the middle position that is hard to analyze as a cantilever column (Mo and Wang, 2000). Figure 7 points out the difference. Supposed a torsion-spring was set on the top of the wing-wall, it is called a semi-rigid frame model. The inflection point moves to the higher position which is caused by the semi-rigid constraint and the real accord (Hseu et al., 1986). From the above concept, the inflection point was first found and the rigidity and strength of the specimen from KH as an effective height was then calculated.

Effective height of wing-wall

Deformation and bending moment of the specimen under the lateral force and axial force were shown in Figure 8. Supposed the base of the wing-wall was fixed, the moment that causes the inflection point of a specimen on the base would be KPH. Top bending moment should be PH (1-K) , and the ultimate lateral force is Pu.

Supposing:

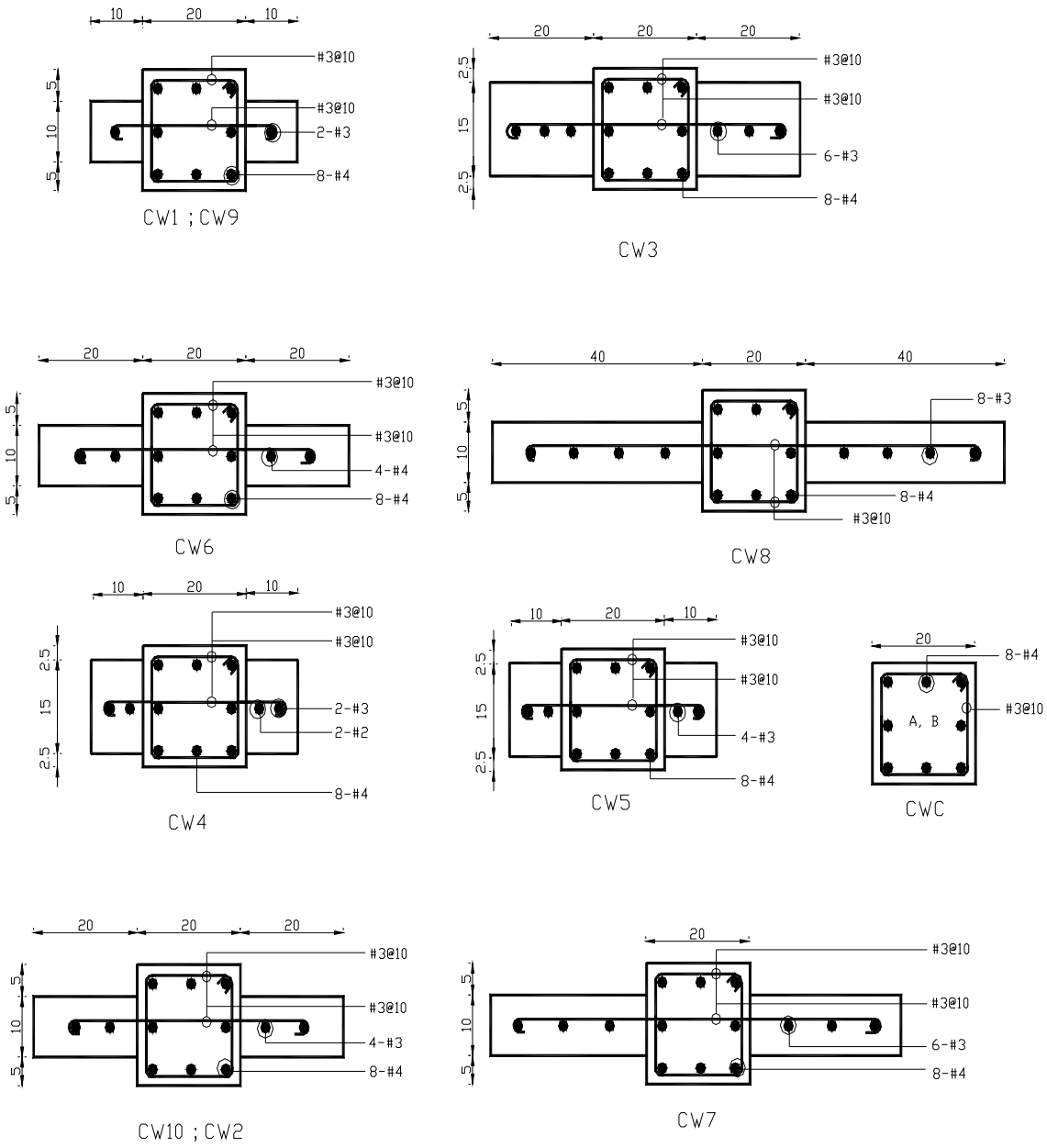

Figure 2. Steel arrangement in wing-wall specimen (unit : cm).

$$P_u H - M_T = M_u \quad (1)$$

$$P_u H - (1-K) P_u H = M_u \quad (2)$$

$$K P_u H = M_u \quad (3)$$

At the ultimate bending moment (Mu), the lateral force (Pu) can be found either from the effective height in equation (3) that is divided (Mu) by the test result (Pu) which is further calculated from reinforced concrete theory. Table 2 shows the effective height of the specimen with which the ultimate moment (Mu) is bore and factor k can be found from an experiment rule, that is:

$$\mathrm{K} = \frac{(B_c + B_w + D_c + 2.5D_w)}{\sqrt{94 \times (B_c + B_w + D_c + D_w)^2 \times \frac{f_c}{f_{yw}}}} \quad (4)$$

The coefficients in equation (4) are as follows:

Bc, column thickness; Bw, wing-wall thickness; Dc, column width; Dw, elongation width of a wing- wall; fyw, yielding stress of steel in wing-wall; and f'c, compressive strength of concrete.

From experimental rule, inflection point factor (K) can be calculated. The cracking bending moment from the theory's specimen (Mcr), the yielding bending moment (My) and the ultimate bending

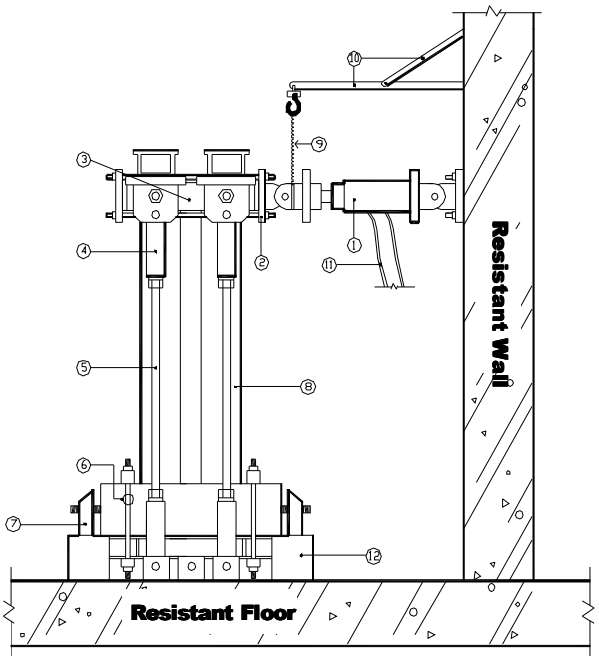

Figure 3. Test frame and hinge fixed bars for wing-wall test sets.
Note: 1. Actuator 2. Connecter between actuator and test frame sets 3. Sets of cap 4. Connecter between cap and specimen 5. Vertical rod for fixed cap 6. Rod for fixed specimen based on test frame 7. Anti-lateral drift board 8. Specimen 9. Hang-tie for actuator 10. Frame for actuator 11. High pressure oil cable 12. Test base.

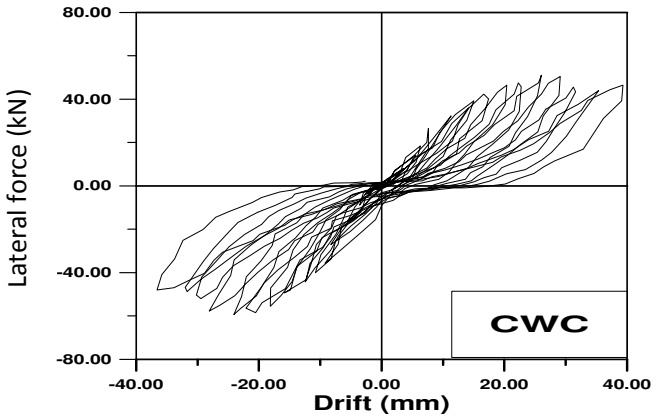

Figure 4. Lateral force-drift relative diagram of a single column specimen.

moment (Mu) that was reversed and used in calculating the mean time force, caused the cracking force (Pcr), yielding force (Py) and ultimate force Pu. The results are shown in Tables 3, 4 and 5.

Though, the factor induced results that are not suitable in Tables 3 and 4, it showed the experimental factor K used in calculating (Py). Consequently, when this was compared to the test result, the tolerance decreased to about 20%. In the ultimate stage, in the same way, the tolerance almost decreased to 10% in Table 5 which

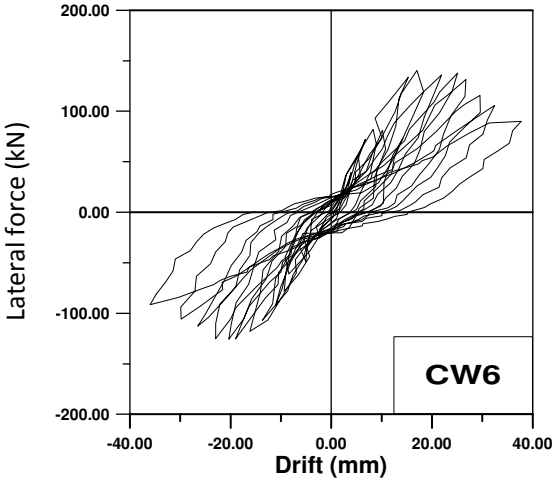

Figure 5. Drift-lateral force relation of wing-wall.

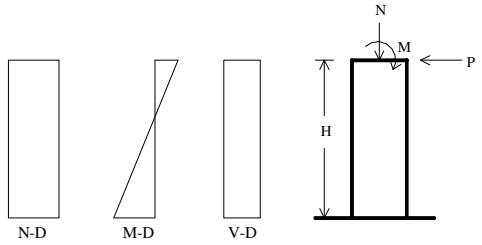

Figure 6. Axial load diagram, shear diagram and bending moment diagram of a specimen under external force.

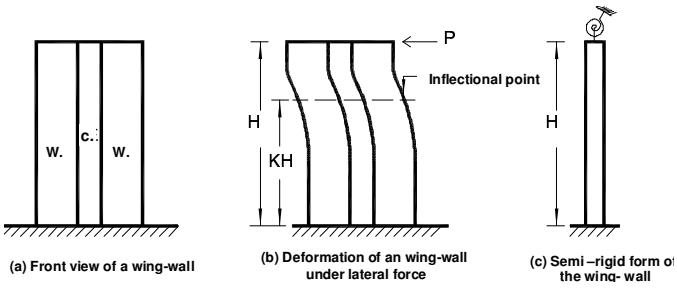

Figure 7. Wing-wall modified as a semi-rigid frame.

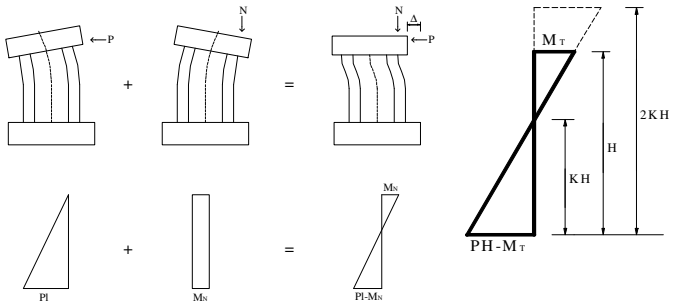

Figure 8. Deformation by bending moment of specimen.

Table 1. Size of specimens and steel arrangement.

S	Size		fc'(mpa)	Steel arrangement	Wall ρ (%)
	T (cm)	W (cm)			
CWC	-	-	18.1	-	-
CW1	10	10	18.1	1-#3	0.71
CW9			23.38	1-#3	0.71
CW2			16.17	2-#3	0.71
CW6		20	16.17	2-#4	1.26
CW10			23.38	2-#3	0.71
CW7		30	18.1	3-#3	0.71
CW8		40	16.17	4-#3	0.71
CW4	15	10	18.1	1-#2,1-#3	0.69
CW5			18.1	2-#3	0.95
CW3		20	18.1	3-#3	0.71

Note: 1. Wing-wall column section 20cm*20cm, main bars 8-#4 , # 4, steel fy = 575.68Mpa. 2. Wall longitudinal steel #3, fy = 430.39 Mpa. 3. The loading type: repeat reversal and increased loading type. 4. S: specimen, T: thick, W: width.

Table 2. Factor K count from theory Mu and test Pu.

S	Mu (kN-cm)	Pu (kN)	K	ex. K
CWC	3683.78	59.39	0.59	0.58
CW1	5624.35	100.8	0.53	0.63
CW9	6335.35	116.61	0.52	0.55
CW2	9047.65	124.23	0.69	0.76
CW6	12416.37	140.37	0.84	0.88
CW10	10918.38	131.9	0.79	0.63
CW7	15493.39	197.23	0.75	0.79
CW8	21715.48	224.73	0.92	0.89
CW4	6951.77	105.02	0.63	0.62
CW5	7319.67	112.82	0.62	0.62
CW3	12965.81	175.78	0.70	0.70

Note: S: specimen, ex.: experiment.

Table 3. From experiment K to calculate theory Pcr.

S	Mcr (kN-cm)	T1 Pcr (kN)	Test Pcr (kN)		T2(%)	
			pu.	dr.	pu.	dr.
CWC	353.2	6.96	13.7	16.7	49.1	58.2
CW1	794.7	12.89	20.6	21.6	37.3	40.2
CW9	902.6	16.41	22.5	25.5	27.0	35.6
CW2	1561.	20.42	35.3	35.3	42.1	42.1
CW6	1561.	18.98	41.2	22.5	53.9	15.6
CW10	1872.	29.05	29.4	41.5	1.1	29.9
CW7	2869.	35.91	93.1	90.1	61.4	60.1
CW8	4198.	46.62	81.3	68.6	42.6	32.0
CW4	1103.	17.80	21.6	21.6	17.5	17.5
CW5	1103.	18.01	15.7	29.4	-14.	38.7
CW3	2413.	33.59	45.1	39.2	25.5	14.3

Note: S: specimen, T1: theory, T2: tolerance Pu: push, dr. draw.

Table 4. From experiment K to calculate theory Py.

S	My (kN-cm)	T1 Py (kN)	Test Py (kN)		T2 (%)	
			pu.	dr.	pu.	dr.
CWC	3415.3	55.96	40	42	39.9	33.2
CW1	3393.05	51.43	60.5	71	14.9	27.5
CW9	3600.22	61.97	78.9	89.4	21.4	30.7
CW2	5543.66	69.43	79.8	87.2	12.5	20.4
CW6	9497.96	102.88	94.7	78.9	8.64	30.3
CW10	6060.03	91.27	84.2	94.7	8.40	3.62
CW7	8799.71	106.71	130	130	17.9	17.9
CW8	12283.61	131.88	136.	168	3.62	21.5
CW4	3966.45	61.06	76.4	76.4	20.1	20.1
CW5	4271.03	65.75	73.6	65	10.7	1.15
CW3	7068.44	95.66	105	94.7	8.90	1.01

Note: S: specimen, T1: theory, T2: tolerance, pu: push, dr. draw.

Table 5. From experiment K to calculate theory Pu.

S	Mu	T1	Test Pu (kN)		T2 (%)	
	(kN-cm)	Pu(kN)	pu.	dr.	pu.	dr.
CWC	3683.78	60.36	51.0	59.4	-18.3	-1.63
CW1	5624.35	85.25	95.3	100.	10.5	15.4
CW9	6335.35	109.1	105.9	116.6	-2.94	6.48
CW2	9047.65	113.3	117.3	125.	4.19	-6.87
CW6	12416.3	134.5	140.3	125.	4.19	-6.87
CW10	10918.4	164.5	131.6	131.	-24.9	-24.6
CW7	15493.4	187.9	197.2	197.	4.74	4.64
CW8	21715.5	233.1	224	238	-3.74	-2.38
CW4	6951.8	107.0	105.	101.	-1.9	-5.8
CW5	7319.7	112.7	112.8	98.7	0.12	-14.1
CW3	12965.8	175.5	175.8	170.	0.17	-2.77

Note: S: specimen, T1: theory, T2: tolerance pu: push, dr. draw:

showed that factor K is worth using.

Deflection rigidity analysis

Wing-wall was composed by column and walls. The structural behavior of a wing-wall is similar to that of the element behavior of the beam-column that includes cracking, yielding, ultimate and four steps of rupture. Further, lateral force of each step was defined as that force which made the specimen cracking out (as cracking force), the steel yielding (as yielding force) and the strain of the concrete reach 0.003 in compressive zone or the steel strain reach 0.002 as the ultimate bearing of the specimen. Figure 8 points to the moment diagram of a specimen under lateral force and uses the conjugate beam method concept to find out the height change as the rigidity change of the specimen. The formulas will be shown as follows when one fixed end and another end are used to constrain the torsion spring of a column.

$$\overline{M} = (\frac{1}{2} * KH * \frac{PKH}{E_C I}) * (1 - \frac{K}{3})H - \left[\frac{1}{2}(1-K)H * \frac{P(1-K)H}{E_C I}\right] * (\frac{1-K}{3})H \quad (5)$$

$$\Delta = \overline{M} = (\frac{3K-1}{2})(\frac{PH^3}{3E_C I}) = \frac{(3k-1)PH^3}{6E_c I} \quad (6)$$

The factors in equations (5) and (6) are shown as follows:

K, the ratio of the inflection point height to the height of the specimen.
P, the lateral force acts on the top of a specimen.
EC, the modulus of concrete material.
EC, 15000√fc(kg/cm2) = 4696.68√fc(Mpa).
I, rigidity of specimen.

The wing-wall is different in the section area and steel arrangement. Its deformation under lateral force and theory rules the Mcr , My , Mu and K. Consequently, there will be some difference in various stages. The way of calculating specimen's deformation will be as follows:

As lateral force P≦Pcr

$$I = I_g \quad (7)$$

$$\Delta = \frac{(3k-1)PH^3}{6E_c I_g} \quad (8)$$

As lateral force Pcr < P < Py. According to ACI Code, the moment of inertia and deformation formula was used as follows :

$$I_{eff} = (\frac{M_{cr}}{M_{\max}})^3 I_g + \left[1 - (\frac{M_{cr}}{M_{\max}})^3\right] I_{cr} \leq I_g \quad (9)$$

$$\Delta = \frac{(3k-1)PH^3}{6E_c I_{eff}} \quad (10)$$

As Pu > P > Py,

$$I = 0.1 I_{cr} \quad (11)$$

$$\Delta = \frac{(3k-1)PH^3}{6E_c I_{cr}} \quad (12)$$

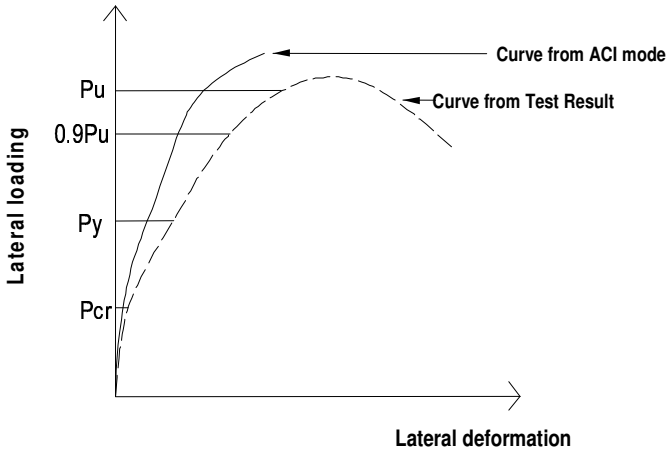

Figure 9. The comparison between test result and result from ACI code calculated.

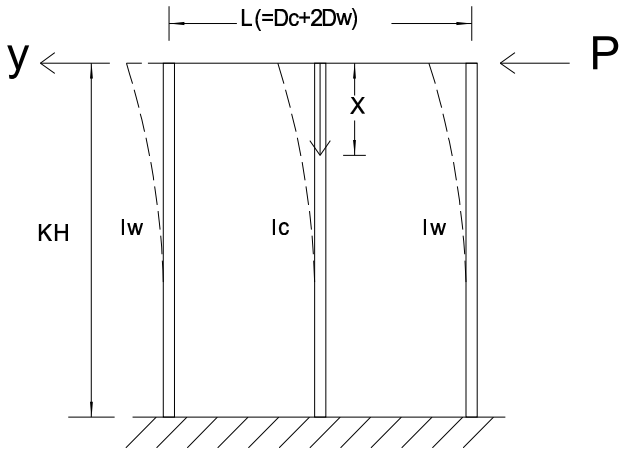

Figure 11. Modified I model of wing-wall and wing-wall drift under lateral force.

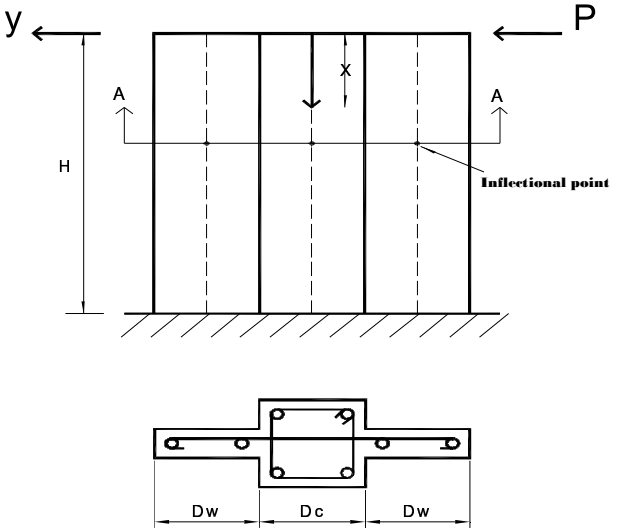

Figure 10. Front view of specimen section A-A.

The P-△ curve of the test result was compared with the result from formulas (8), (10) and (12) and was shown in Figure 9.

The modified rigidity of wing-wall for real behavior

Calculating the rigidity of the wing-wall before modifying revealed that the rigidity is higher than pre-yielding in real testing. The reason is that wing-wall contributed an effective performance in seismic resistance, but the effective rigidity of the wing and column was a little different. Also, the wing-wall promotes efficiency in seismic resistance, but the interaction between column and wall was considerable. As a result, an adept modification is needed. Figures 9, 10 and 11 reveal that the real interactions between the concept "Ig=Ic+2Iw" should be modified as follows:

$$Igm=Ic+\eta(2Iw) \quad (13)$$

Igm : - the modified section moment of inertia

Ic : - the modified cracking section moment of inertia

η : - the influent factor caused by the interaction between the wall and column

The modified P-△curve pre-yielding

The yielding of a column defined as the column outer steel reached yielding, but was not suitable for the wing-wall and outer layer steel which should have reached yielding in wing before the column of awing-wall. As a result, the wing-wall will not be at a plastic hinge stage before the column outer steel reached the yielding of a wing-wall (Lefas and Kotsovos, 1990). For the fact that the soften phenomena did not happen immediately at the first yielding of a steel in wing-wall, the reversed method derived Py which was made from My as a lateral force. This caused the yielding point that seems to be pre-yielding from the test vision. Finding the reasonable P-△curve from the theory did not hesitate in decreasing the rigidity to 0.1 Icr just as the yielding state. Controversially, as the lateral force (P) reached 0.9Pu, the deflection rigidity decreased to 0.1 Icr. Consequently, this would be just for the real test reaction. So, the rigidity can be modified to adapt to the model of wing-wall and be expressed as:

1. If lateral force P≦Pcr is the moment of inertia

$$I = I_{gm}$$

$$\Delta = \frac{(3k-1)PH^3}{6E_cI_{gm}} \quad (14)$$

2. When Pcr < P < 0.9Pu is the rule of ACI code:

$$I_{eff} = (\frac{M_{cr}}{M_{\max}})^3 I_g + \left[1 - (\frac{M_{cr}}{M_{\max}})^3\right] I_{cr} \leq I_g \quad (15)$$

$$\Delta = \frac{(3k-1)PH^3}{6E_cI_{effM}} \quad (16)$$

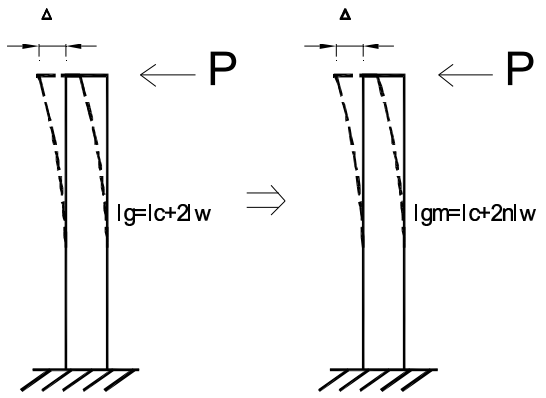

Figure 12. Cantilever model of wing-wall under inflection point

3. When lateral force Pu > P > 0.9Pu

$$I = 0.1 I_{crm} \tag{17}$$

$$\Delta = \frac{(3k-1)PH^3}{6E_c(0.1I_{crm})} \tag{18}$$

In the residual stage of a specimen test, secant stiff rigidity was used as stiffness of a specimen 0.1Icrm and as a decreased gap and the final stage was used as the total deformation reaching 1.5 times ultimate deformation (△u).

Shear behavior of wing-wall

Calculation of shear strength of wing-wall

Figure 12 reveals the interaction of a wing-wall component wall and column that modified cantilever element model, which is more suitable for a specimen deformation under lateral force. In lateral force to deformation relation, the deformation quantity in X direction under inflection point of a specimen can be calculated by formula (19) as suggested by Timoshenko S. P (Timoshenko and Goodies, 1970), that is:

$$\delta = \frac{PX^3}{6E_C I} - \frac{PXH^2}{2E_C I} + \frac{PH^3}{3E_C I} + \frac{P(\frac{L}{2})^2}{2GI} * (H - X) \tag{19}$$

As X = 0 , , the deformation at the top of cantilever column can be calculated as formula (20) and shear deformation will be calculated as formula (21):

$$\delta = \frac{PH^3}{3E_C I} + \frac{P(\frac{L}{2})^2}{2GI}(H) \tag{20}$$

$$\delta_s = \frac{P(\frac{L}{2})^2}{2GI}(H) \tag{21}$$

Table 6. The comparison of shear force Vu from the calculated test result of wing-wall.

S	T1	Test Pu (kN)		T2 (%)	
	Vu (kN)	pu.	dr.	pu.	dr.
CWC	69.09	51.0	59.4	35.3	16.3
CW1	124.0	95.3	100.	30.1	23.0
CW9	132..9	105.9	116.6	25.4	14.
CW2	131.9	117.3	125.	12.4	6.17
CW6	138.1	140.3	125.	1.57	9.79
CW10	152.1	131.6	131.	15.6	15.3
CW7	183.7	197.2	197.	6.86	6.76
CW8	205.7	224	238	8.47	8.47
CW4	124.8	105.	101.	18.9	23.4
CW5	134.3	112.8	98.7	18.9	35.8
CW3	158.6	175.8	170.	9.78	7.12

Note: S: specimen, T1: theory, T2: tolerance pu.: push, dr: draw

The shear deformation of a wing-wall will be calculated as:

$$\delta_s = \frac{P(\frac{L}{2})^2}{2GI}(KH) = \frac{PL^2 KH}{8GI} \tag{22}$$

According to ACI code, the ultimate shear force of a reinforced concrete element can be calculated by the following :

Vu=Vc+Vs (23)

Vu : - ultimate shear force of reinforced concrete element.

Vc : - ultimate shear force of concrete.

Vs : - ultimate shear force of steel.

Table 6 reveals that the test results of the wing-wall's shear force is accommodated with the theory result from formula (23) when the width of the wall is greater and the resistant ability is evident.

Modified shear rigidity of wing-wall

Shear rigidity (GA) of an element varies with the element in different stage of breaking. Also, it is evident that the effective shear area (Ashr) and Possion's ratio (v) vary with different stage of breaking, too. Shear modulus of concrete (Gc) and the effective shear section (Aeff) can be calculated as follows:

$$G_C = \frac{E_C}{2(1+\nu)} \tag{24}$$

v : Possion's ratio 0.3

$$A_{shr} = \frac{A_{gt}}{f_a} \tag{25}$$

fa : - shape factor of an element, wing-wall as 1

Tangent shear rigidity (GAtan) calculated as:

GAtan = GcAshr (26)

The modified rule for each stage is as follows:

Elastic stage : and tangent shear rigidity (GAtan).

Cracking stage : and tangent shear rigidity (GAtan) discount 1/3 as elastic stage.

Ultimate stage: tangent shear rigidity (GA) as 0.

DISCUSSION ON TEST RESULTS

A wing-wall deformation under lateral force can be divided into deflection and shear deformation in further discussions (Ohmiya and Hayashi, 2000). The deflection deformation under lateral force can be calculated as formula (18) and shear deformation can be calculated as formula (22). Then, the whole deformation (ΔT) of a specimen will be as follows:

$$\Delta_T = P[\frac{(3K-1)H^3}{6E_C I} + \frac{PL^2 KH}{8GI}] \quad (27)$$

With the change in stage and different condition, the calculated equation will be followed. The test results will be compared with the results from equation (27):

(1). When the width of a single wing is less than that of a column. Table 7 reveals great tolerance between test result and result from the theory before cracking stage (Pcr) . Table 8 reveals less tolerance in yielding stage. In the ultimate stage, the tolerance between test result and result from the theory will be much lesser than that in the further stage as the result reveals from Table 9.
(2). The tolerance between test and calculated results is greater when the width of the single wing is greater than that of the column at the cracking stage. This is revealed in Table 10. Gradually, the tolerance decrease when it gets to the yielding stage and becomes much lesser when it gets to the ultimate stage. Tables 11 and 12 revealed the results evidently.

The reason for further results from the test and the conducted action phenomena was not considered. Particularly, the elongation effect from long steel should have great influent effects. The resistance promotes the ratio that is increasing both the width of the wall and column. The relation can be found from Table 13 and Figure 13. Also, if the relation that is almost in scale decreases one time, the resistant force will promote two times. In the mean time, increasing the steel ratio will promote the resistant force, either way. In the specimen, CW6 reveals the result.

Table 7. The comparison of Pcr and △cr with the width of the wall smaller than that of the column.

S	Pcr (kN)			△cr (mm)		
	T1	test	T2 (%)	T1	test	T2 (%)
CWC	6.96	13.7	-49.2	0.79	2.8	-71.8
CW1	12.89	20.6	-37.4	0.72	1.33	-45.9
CW9	16.41	22.5	-27.1	0.62	2.14	-71.1
CW4	17.79	21.6	-17.6	0.85	2.1	-59.5
CW5	18.0	15.7	14.6	0.86	0.9	-4.44

Note: S: specimen, T1: theory, T2: tolerance.

Table 8. The comparison of Py and △y with the width of the wall smaller than that of the column.

S	Py (kN)			△y(mm)		
	T1	test	T2 (%)	T1	test	T2 (%)
CWC	50.33	42.0	19.8	7.35	16.6	-55.72
CW1	51.4	60.5	-15.0	5.19	8.9	-41.69
CW9	61.99	78.9	-21.4	4.32	12.5	-65.44
CW4	61.02	76.4	-20.1	5.56	9.5	-41.47
CW5	65.71	65.0	1.0	5.99	8.5	-29.53

Note: S: specimen, T1: theory, T2: tolerance.

Table 9. The comparison of Pu and △u with the width of the wall smaller than that of the column.

S	Pu (kN)			△u(mm)		
	T1	test	T2 (%)	T1	test	T2 (%)
CWC	60.36	59.4	-0.1	24.78	39.3	-36.9
CW1	85.25	95.3	-11.0	21.92	37.0	-40.8
CW9	10.91	105.9	2.68	19.0	37.6	-49.5
CW4	107.0	105.0	1.69	25.34	35.7	-28.9
CW5	112.8	112.8	-0.54	26.58	35.1	-24.2

Note: S: specimen, T1: theory, T2: tolerance.

Table 10. The comparison of Pcr and △cr with the width of the wall greater than that of the column.

S	Pcr (kN)			△cr(mm)		
	T1	test	T2 (%)	T1	test	T2 (%)
CW2	20.43	35.3	-42.12	0.69	0.96	-28.1
CW6	19.39	22.5	-13.82	0.78	0.97	-1.58
CW10	29.06	29.4	-1.15	0.61	0.89	-31.5
CW7	35.89	90.1	-60.16	0.53	3.4	-84.4
CW8	46.63	68.6	-32.02	0.46	1.98	-76.8
CW3	33.75	39.2	-14.36	0.69	2.38	-71.0

Note: S: specimen, T1: theory, T2: tolerance.

Conclusions and Suggestion

From the test results, the seismic resistance of wing-wall was seen as a special characteristic found to be

Table 11. The comparison of Py and △y with the width of the wall greater than that of the column.

S	Py (kN)			△y(mm)		
	T1	test	T2 (%)	T1	Test	T2 (%)
CW2	69.45	79.4	-12.53	7.72	10.4	-25.8
CW6	105.0	94.7	10.9	11.12	8.9	24.9
CW10	91.3	84.2	8.42	6.56	8.6	-23.7
CW7	106.6	130	-17.97	6.94	9.9	-29.9
CW8	131.9	136.8	-3.61	6.51	7.6	-14.3
CW3	95.6	94.4	0.95	7.75	7.2	7.64

Note: S: specimen, T1: theory, T2: tolerance.

Table 12. The comparison of Pu and △u with the width of the wall greater than that of the column.

S	Pu (kN)			△u(mm)		
	T1	test	T2 (%)	T1	test	T2 (%)
CW2	113.3	117.3	-3.51	31.0	28.8	7.75
CW6	134.5	140.4	-2.26	32.4	37.8	-14.2
CW10	164.5	131.9	24.32	29.3	40.0	-26.7
CW7	187.9	197.0	-4.75	29.3	30.1	-2.62
CW8	233.1	238.8	-2.54	26.4	26.2	0.46
CW3	175.5	175.8	-0.48	38.6	28.2	36.9

Note: S: specimen, T1: theory, T2: tolerance.

Table 13. Scale ratio of wall to column compared with the lateral resistant force in wing-wall.

Specimen	W	R1	Pu (kN)	R2
CWC	-		59.39	1
CW1	10	0.5	100.28	1.69
CW9	10		116.6	1.96
CW2	20		124.2	2.09
CW6	20	1	125.9	2.11
CW10	20		131.9	2.22
CW7	30	1.5	197.0	3.31
CW8	40	2	224.7	3.78
CW4	10	0.5	105.0	1.77
CW5	10		112.8	1.89
CW3	20	1	175.8	2.95

Note: W: width of one side of the wall (cm). R1: scale ratio of one side of the wall to column. R2: resistant force ratio of specimen to single column

semi-rigid. Consequently, the variance of effective height of a specimen will influence the seismic resistance. The interaction between wall and column exists from the fact that the real characteristic of wing-wall rigidity is softer than that of the two department wall, including the column.

The width and thickness of the wall in a wing - wall specimen decide the seismic resistance ability of a wing-wall specimen. The relations among these factors are:

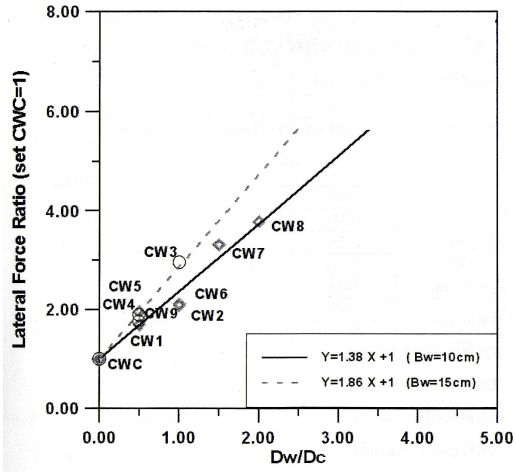

Figure 13. The relations between the width and resistance promotion of the wing-wall.

The width of one side of the wall is the double size of the column, while the resistance of lateral force will promote two times the resistant force. The conclusion is similar with that from the JCI (Japan Concrete Institute, 1984).

The resistant shear force increased once as the single column for the wall's width increased to 100 mm. The resistant shear force even increased for about four to five times as the single column did when the width of the wall is two times the single column.

With the same section area, the better seismic resistance will be shown in the wall that has a wider width than a thicker thickness.

The wall area and width is greater than a single column whose seismic resistance is evident and effective.

There are many advantages in using seismic resistant for the performance of wing-wall. Consequently, there is need to set up a more detailed mechanism for the accommodation design and its feasible usage.

ACKNOWLEDGEMENTS

The authors would like to thank the National Science Council of the Republic of China, Taiwan, for their financial support of this research under Contract Nos. NSC 99-2628-E-153-001 and NSC 98-2221-E-153-004. The authors are also most grateful for the kind assistance of Prof. Huisheng Peng (Editor of IJPS) and the constructive suggestions of the anonymous reviewers, all of which led to the making of several corrections and suggestions that improved the presentation of this paper.

REFERENCES

Chen CW (2006). Stability Conditions of Fuzzy Systems and Its

Application to Structural and Mechanical Systems, Advances in Engineering Software, Vol. 37, No. 9, pp. 624-629, Sep
Chen CW, Lin CL, Tsai CH, Chen CY, Yeh K (2007). A Novel Delay-Dependent Criteria for Time-Delay T-S Fuzzy Systems Using Fuzzy Lyapunov Method, Int. J. Art. Intell. Tools, 16(3): 545-552.
Chen CW (2009). Modeling and control for nonlinear structural systems via a NN-based approach, Exp. Syst. Appl., 36(3): 4765-4772.
Chen PC, Chen CW, Chiang WL (2009). GA-based modified adaptive fuzzy sliding mode controller for nonlinear systems, Exp. Syst. Appl., 36(3): 5872-5879.
Chen CW, Ken Y, Liu FR (2009). Adaptive fuzzy sliding mode control for seismically excited bridges with lead rubber bearing isolation, Int. J. Uncertainty, Fuzziness Knowledge-Based Syst. 17(5): 705-727.
Chen CW (2009). The stability of an oceanic structure with T-S fuzzy models, Math. Comp. Simulation, 80(2): 402-426.
Chen CY, Lin JW, Lee WI, Chen CW (2010). Fuzzy control for an oceanic structure: A case study in time-delay TLP system. J. Vib. Cont., 16(1): 147-160.
Chen CW (2010). Modeling and fuzzy PDC control and its application to an oscillatory TLP structure, Math. Problems Eng.- An Open Access Journal, 13: Doi: 10.1155/2010/120403.
Chen CW, Shen CW, Chen CY, Jeng MJ (2010). Stability analysis of an oceanic structure using the Lyapunov method, Eng. Comp., 27(2): 186-204.
Chen CW, Chen PC (2010). GA-based adaptive neural network controllers for nonlinear systems, Int. J. Innov. Comput. Inform. Contr. 6(4): 1793-1803.
Mo YL, Wang SJ (2000). Seismic Behavior of Reinforced Concrete Column with Various Tie Configurations, J. Struc. Eng. pp. 1122-1130.
Hseu MS, Huang CC, Kuo HM (1986). Experimental and Theoretical Study of Low-Rise Reinforced Concrete Shear Wall Without Boundary Elements, 7th Annual Meeting of Japanese Association for Earthquake Engineering, Tokyo, Japan., pp 12.
Lefas ID, Kotsovos MD, Ambraseys NN (1990). Behaviour of reinforced concrete structural walls: strength, deformation, characteristics, and failure mechanism. ACI Struct. J. 87(1): 23-31.
Lefas ID, Kotsovos MD (1990). Strength and deformalion characteristics of reinforced concrete walls under load reversals. ACI Struct. J. 87(6): 716-726.
Timoshenko SP, Goodies JN (1970). “Theory of Elasticity”, McGraw-Hill Book Company, New York. p. 46.
Ohmiya M, Hayashi S (2000). Shear and Flexural Strength of Columns with Wing Walls, 25th Conference of On our World in Concrete and Structures. Singapore, 493-500.
Japan Concrete Institute (JCI) (1984). A study on the Seismic Strengthening of the Existent R.C Constructions, Japan.